

ROBUST ACTIVE CONTROL LAW WITH INTERNAL MODEL FOR VIBRATION ATTENUATION

Eliza MUNTEANU¹, Ioan URSU²

Lucrarea de față continuă o serie de cercetări ale autorilor ([1], [2]) în domeniul controlului activ al vibrațiilor pentru un model de aripă din material compozit prin utilizarea de actuatori piezo de tip MFC (Macro-Fiber-Composite). Caracteristicile de robustețe ale controlului optimal LQR (Linear Quadratic Regulator) sunt recuperate de către filtrul Kalman aplicând o construcție specială a estimatorului. Legea de control obținută poartă numele de LQG/LTR (Linear Quadratic Gaussian/ Loop Transfer Recovery). Pe de altă parte, introducerea unui model intern în compensatorul sistemului oferă un plus de robustețe și performanțe remarcabile.

The present work continues some recent researches of the authors ([1], [2]) in the vibration active control domain for a composite wing model by using MFC (Macro-Fiber-Composite) piezo actuators. The robustness characteristics of the optimal control LQR (Linear Quadratic Regulator) are recovered by the Kalman filter applying a special construction for the estimator. The obtained control law is called LQG/LTR (Linear Quadratic Gaussian/ Loop Transfer Recovery). Moreover, including an internal model in the compensator of the system confers more robustness properties and remarkable performances.

Keywords: robust active control, composite wing, MFC piezo actuators

1. Introduction

In general, to meet the regulatory requirements for any certified aircraft to be free of wing dangerous vibrations, one can use either passive or active control techniques. The first ones increase the structure weight and in certain situations are not feasible. The active techniques enhance dynamic behavior of the wing, without redesign and adding mass; nowadays, these are used both for flutter suppression and structural load alleviation. Thus, herein our target concerns the obtaining of a robust active control law, based on the LQG/LTR synthesis [3], for a piezo smart composite wing. Moreover, to increase the robustness characteristics and the performance of the designed control law we incorporate an

¹ PhD Student eng., Advanced Studies and Research Center, România, email: eliza.munteanu@asrc.ro

² PhD. math., National Institute for Aerospace Research “Elie Carafoli”, România, email: iursu@incas.ro

internal model [4].

The organization of the paper is as follows. Section 2 presents the mathematical model derived from an ANSYS FEM (Finite Element Method) structural modeling. Section 3 presents a design of the LQG/LTR scheme of control synthesis. Section 4 ends the work with numerical simulations and Section 5 present some conclusions.

2. Mathematical model

The computational program ANSYS, performing FEM analysis of a wing physical model defined only in terms of geometrical and structural data [5], was applied to obtain the structural, second order, mathematical model

$$M\ddot{x} + Kx = 0 \quad (1)$$

where x is the vector of nodal displacements, and M , respectively K are mass and stiffness matrices. A model wing with an Eppler 211 airfoil and basic dimensions semi-span - 650 mm and chord - 200 mm, was considered. The wing skin is built from a composite material E-glass texture/ortho-ophthalic resin with 4 layers and 0.14 mm thickness each. The wing spars, placed at 30 %, respectively, 65 % of chord, are made of the same material, but with different number of layers. The ANSYS geometric model equipped with MFC (Macro Fiber Composite) actuators is given in Fig. 1. The skin and the spars were modeled as *shell 99* - 2D - elements. In fact, the wing skin with MFC S1 actuators has five layers (four layers for composite material and one layer for MFC materials).

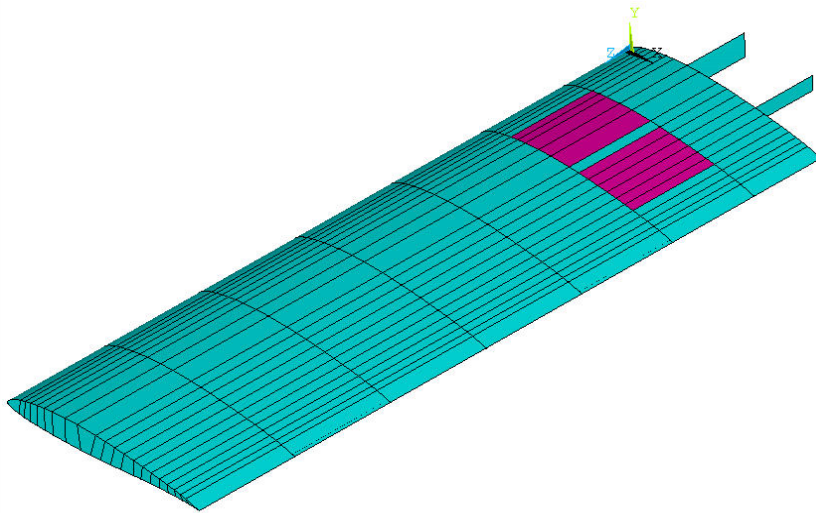


Fig. 1. The wing model with two pairs of MFC

(one pair for introducing the perturbation and one pair for the control signal)

MFC S1 is a smart piezoelectric actuator with collocated sensor that has been developed at the NASA Langley Research Center. It is composed of rectangular fibers diced from a piezoceramic wafer. The main advantage of fiber-based actuators is their poling in the same direction as their length. Thus, they are able to act with the piezoelectric strain constant d_{33} that is about twice as much as the d_{31} constant, used to actuate conventional PZT patches, which are poled in a direction transverse to their length [6].

Following a modal analysis using the full ANSYS model, the first three natural modes and frequencies (Hz) – 18.98, 79.58 and 327.78 – were found.

Then, by an ANSYS substructuring analysis, the mathematical model was completed in the form

$$M\ddot{x} + Kx = \tilde{B}_1\xi + \tilde{B}_2u \quad (2)$$

where \tilde{B}_1, \tilde{B}_2 are the vectors of the influences of the perturbation ξ and the control u . The operation assumed the static interaction cause-effect

$$Kx_k = \tilde{B}_2u_k, Kx_k = \tilde{B}_1\xi_k, \quad (3)$$

x_k being the displacement vector corresponding to a unitary electric field u_k applied to the k MFC actuator. In principle, to calculate piezo action, we used the analogy between thermal and piezoelectric equations developed in [8], so introducing a thermal model for piezo material. Analogously one proceeds for obtaining of the vector \tilde{B}_1 . The subsequent operations concern a) the recuperation in MATLAB of the matrices in system (2), codified in ANSYS as Harwell Boeing format and b) the modal transformation

$$x = Vq \quad (4)$$

of the system (2) by using a reduced modal matrix (of order three) of eigenvectors V of dimension 7740×3 (7740 is the number of generalized coordinates in ANSYS, in connection with the number of the chosen FEM nodes)

$$V^T M V \ddot{q} + V^T C V \dot{q} + V^T K V q = V^T \tilde{B}_1 \xi + V^T \tilde{B}_2 u \quad (5)$$

Thus, a modal quasidecentralized system, of three modes:

$$\ddot{q} + \text{diag}(2\zeta_i \omega_i) \dot{q} + \text{diag}(\omega_i^2) q = B_1 \xi + B_2 u \quad (6)$$

is obtained as a basis for standard LQG optimal problem, defined in terms of the first order state form system

$$\begin{aligned}\dot{x}(t) &= Ax(t) + B_1\xi(t) + B_2(t)u(t) \\ z(t) &= C_1x(t) \\ y(t) &= C_2x(t) + \mu I\eta(t)\end{aligned}\tag{7}$$

where $x(t)$ is the state, $z(t)$ is the controlled output, $y(t)$ is the measured output, and $u(t)$ is the control input. The state vector is given by

$$x(t) = (q_3, q_2, q_1, \dot{q}_3, \dot{q}_2, \dot{q}_1)^T\tag{8}$$

The external and internal components of the perturbations ξ and η are the substitute of the aerodynamic disturbances and sensor noise vector, respectively. The controlled output $z(t)$, in the following, will concern the whole system state (the modes and the modal derivatives); the control vector variable $u(t)$ will be also penalized, taking into account the definition of the cost, see next Section. After the modal analysis, three displacement and three velocities were assigned for each node from the ANSYS wing model. The y -axis displacement of the node where the sensor is positioned will be taken as measured output $y(t)$.

3. Design of LQG/LTR robust active control

The LQG control synthesis concerns the system (6). The goal is to find a control $u(t)$ such that the system is stabilized and the control minimizes the cost function

$$J_{LQG} = \lim_{T \rightarrow \infty} \frac{1}{T} E \left\{ \int_0^T \begin{bmatrix} x(t)^T & u(t)^T \end{bmatrix} \begin{bmatrix} Q & 0 \\ 0 & R \end{bmatrix} \begin{bmatrix} x(t) \\ u(t) \end{bmatrix} dt \right\}\tag{10}$$

where the operator E denotes expectation (average value). The matrices Q and R are thus defined as

$$Q = C_1^T C_1, \quad R = \rho_R I_2\tag{11}$$

(ρ_R is herein scalar). Thus, the framework of the LQG synthesis is a stochastic one and the minimization of the index (10) means implicitly a minimization of the effect of disturbances on the controlled output z , and, in fact, an active alleviation of the vibrations. The solution is well-known and consists in the building of a controller and a state-estimator (Kalman filter) [8]. The state estimator is of the form

$$\dot{\hat{x}} = A_0 \hat{x}(t) + K_f y(t) \quad (12)$$

The controller makes use of this estimator and is defined by

$$u^*(t) = -K_c \hat{x}(t) \quad (13)$$

The LQG control is built by first solving the decoupled algebraic Riccati equations

$$\begin{aligned} A^T P + PA - PB_2 R^{-1} B_2^T P + C_1^T Q_J C_1 &= 0 \\ AS + SA^T - SC_2^T Q_\eta^{-1} C_2 S + B_1 Q_\xi B_1^T &= 0 \end{aligned} \quad (14)$$

where the noise matrices Q_ξ and Q_η are so defined

$$E \left\{ \begin{bmatrix} \xi(t) \\ \eta(t) \end{bmatrix} \begin{bmatrix} \xi(t) & \eta(t) \end{bmatrix} \right\} = \begin{bmatrix} Q_\xi & 0 \\ 0 & Q_\eta \end{bmatrix} \delta(t - \tau) \quad (15)$$

with $\delta(t - \tau)$ being the Dirac distribution. The controller gain, K_c , the filter gain, K_f , and the filter matrix are defined by

$$K_c = R^{-1} B_2^T P, \quad K_f = S C_2^T Q_\eta^{-1}, \quad A_0 = A - B_2 K_c - K_f C_2 \quad (16)$$

Using the state-estimator (12) and the control law (13), the system (7) becomes

$$\begin{aligned} \dot{x}(t) &= Ax(t) + B_1 \xi(t) - B_2 K_c \hat{x}(t) \\ \dot{\hat{x}}(t) &= K_f C_2 x(t) + K_f \mu I \eta(t) + (A_0 - D_{22} K_c) \hat{x}(t) \end{aligned} \quad (17)$$

As comparison term for this system in numerical simulations, it will be taken the LQR closed loop system

$$\dot{x}(t) = (A - B_2 K_c) x(t) + B_1 \xi(t) \quad (17')$$

and the “passive” one (without control)

$$\dot{x}(t) = Ax(t) + B_1 \xi(t) \quad (17'')$$

Now, in the following, the LQG/LTR procedure will be applied to recover the lost robustness of the LQR system. Indeed, it is well known that the LQR controller has good robustness properties, but these properties are usually lost when the Linear Quadratic Regulator (LQR) is used in conjunction with Kalman filter.

In view of this procedure, both the \mathcal{H}_2 -tradeoff type optimization

perspective used in [3] and the open loop singular value perspective defined in [9], will be involved. Thus, the controller gain synthesis is performed such that

$$C_1(sI - A)^{-1} B_2 / \rho = W(s) \quad (18)$$

where $W(s)$ is a weight to trade the sensitivity function $S(s)$ and complementary sensitivity function $T(s)$

$$S(s) = [I + G(s)K(s)]^{-1}, \quad T(s) = G(s)K(s)S(s) \quad (19)$$

one against the other – WS versus T . It is emphasized that the significance of this functions derives from the following fundamental frequency domain prescriptions for feedback design: a) $S(s)$ must be small whenever output perturbations are large and b) $T(s)$ must be small wherever model errors are large [9]. The filter gain synthesis will be performed such that

$$L_{LQG}(j\omega) \approx L_{LQR}(j\omega) \quad (20)$$

in a certain range, as large as possible $\omega \in [0, \omega_{\max}]$, where ($j\omega = s$)

$$\begin{aligned} L_{LQG}(s) &= \left[-\left(sI - A - K_f C_2 - B_2 K_c \right)^{-1} K_f C_2 \right] (sI - A)^{-1} B_2 \\ L_{LQR}(s) &= K_c (sI - A)^{-1} B_2 \end{aligned} \quad (21)$$

Thus, the filter gain K_f is chosen so that the closed-loop LQG/LTR system (having open loop L_{LQG} transfer matrix, containing Kalman filter matrix) recovers internal stability and some of the robustness properties (gain and phase margins) of the LQR design (with open loop L_{LQR} transfer matrix). In fact, the weight matrix $W(s)$ is chosen such that its crossover frequency is at least the frequency of the first neglected mode.

The internal-model-based approach seems to be the best suited to problems of tracking unknown reference trajectories or rejecting unknown disturbances [4]. Thus, control schemes incorporating a robust controller efficiently address the problem of rejecting all disturbance inputs generated by the exosystem

$$\dot{\xi} = S\xi \quad (22)$$

The dynamics of the introduced compensator, $\theta(t)$, is described by the equation

$$\dot{\theta}(t) = C^* \theta(t) + B^* y(t) \quad (23)$$

where C^* and B^* are weight matrices. The control signal becomes

$$u(t) = -K_0 \hat{x}(t) + K_1 \theta(t) \quad (24)$$

and the LQR and LQG/LTR controlled systems corresponding to the systems (17'), respectively (17) include the compensator's equation (23)

$$\begin{aligned} \dot{x}(t) &= (A - B_2 K_0) x(t) + B_1 \xi(t) + B_2 K_1 \theta(t) \\ \dot{\theta}(t) &= C^* \theta(t) + B^* C_2 x(t) + B^* \mu I \eta(t) \end{aligned} \quad (25)$$

respectively

$$\begin{aligned} \dot{x}(t) &= Ax(t) + B_1 \xi(t) - B_2 K_0 \hat{x}(t) + B_2 K_1 \theta(t) \\ \dot{\theta}(t) &= C^* \theta(t) + B^* C_2 x(t) + B^* \mu I \eta(t) \\ \dot{\hat{x}}(t) &= K_f C_2 x(t) + K_f \mu I \eta(t) + (A - B_2 K_0 - K_f C_2) \hat{x}(t) + B_2 K_1 \theta(t) \end{aligned} \quad (25')$$

The open loop transfer matrices become

$$\begin{aligned} L_{LQG}(s) &= - \left\{ K_0 (sI - A + K_f C_2 + B_2 K_0)^{-1} K_f + \left[K_0 (sI - A + K_f C_2 + B_2 K_0)^{-1} \right. \right. \\ &\quad \left. \left. B_2 + 1 \right] (sI - C^*)^{-1} B^* \right\} C_2 (sI - A)^{-1} B_2 \\ L_{LQR}(s) &= - \left[K_0 - K_1 (sI - C^*)^{-1} B^* C_2 \right] (sI - A)^{-1} B_2 \end{aligned} \quad (26)$$

4. Numerical simulations

The previously described LQG/LTR control synthesis was tested in numerical simulations of the systems (17) in a first step.

We are thus first interested in the passive versus LQG/LTR closed loop systems comparison of the time histories of the three modes, see Fig. 2. By a *trial and error* process, the following values of the LQR and LQG/LTR weighting matrices were chosen

$$\begin{aligned}
Q_J &= \text{diag}(10^7, 10, 10, 10^6, 1, 1), \rho_R = 1 \times 10^{-5} \\
Q_\xi &= q_{csi} B_1 B_1^T, q_{csi} = 1 \\
Q_\eta &= \mu^2 I_1, \mu = 3.16 \times 10^{-10}
\end{aligned} \tag{27}$$

The state perturbation

$$\xi = 500 \sin(2\pi \times f_1 t) \tag{28}$$

was considered as generating a system resonance for the most dangerous, bending type, first mode.

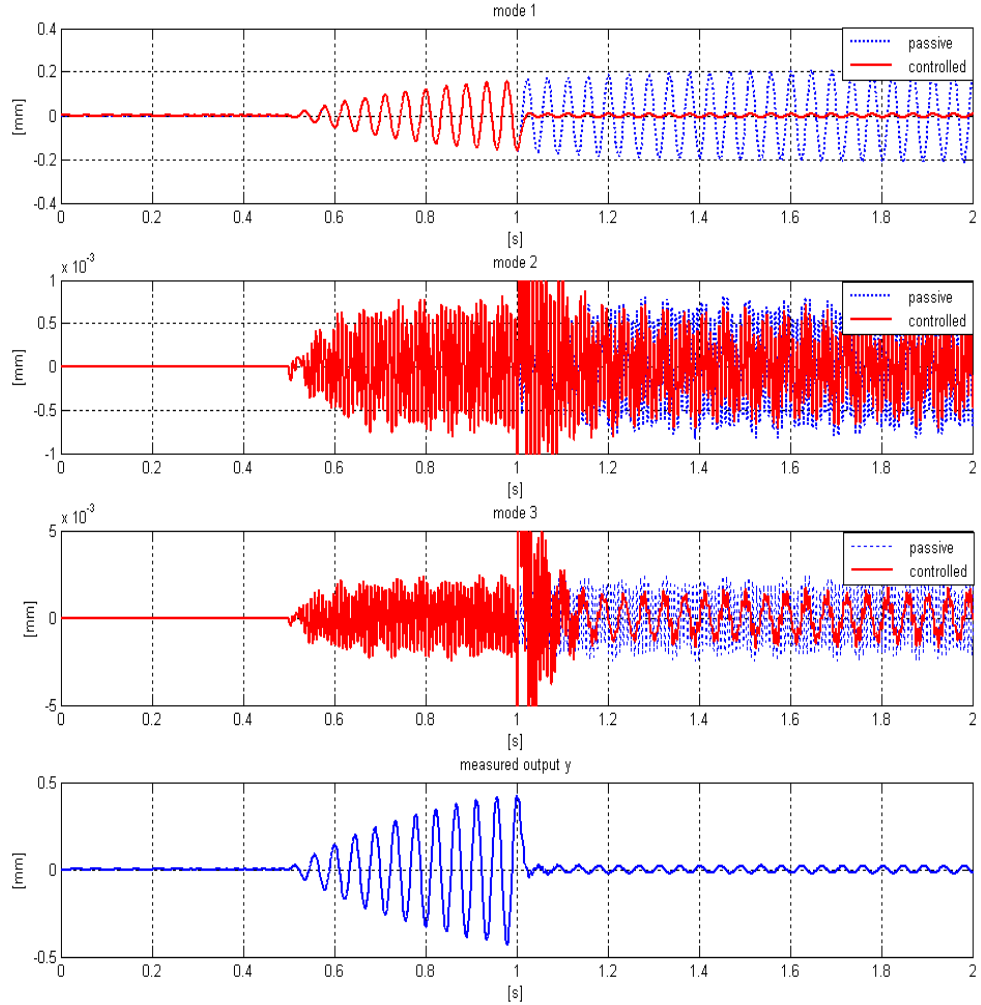


Fig. 2. LQG/LTR closed loop versus passive time histories

Similar sensor noises were introduced

$$\eta = 400 \sin(2\pi \times 50t) \quad (29)$$

The attenuations, in dB values, of LQR and LQG/LTR nominal systems versus the passive one, for the first three modes are: 30.70, -0.72 and -3.53 respectively, 28.60, 2.32 and 3.96 dB. We can remark very close values of the two nominal controlled systems, which means a successful synthesis procedure. On the other hand, the first mode attenuation had a remarkable value and the other two modes remained stable.

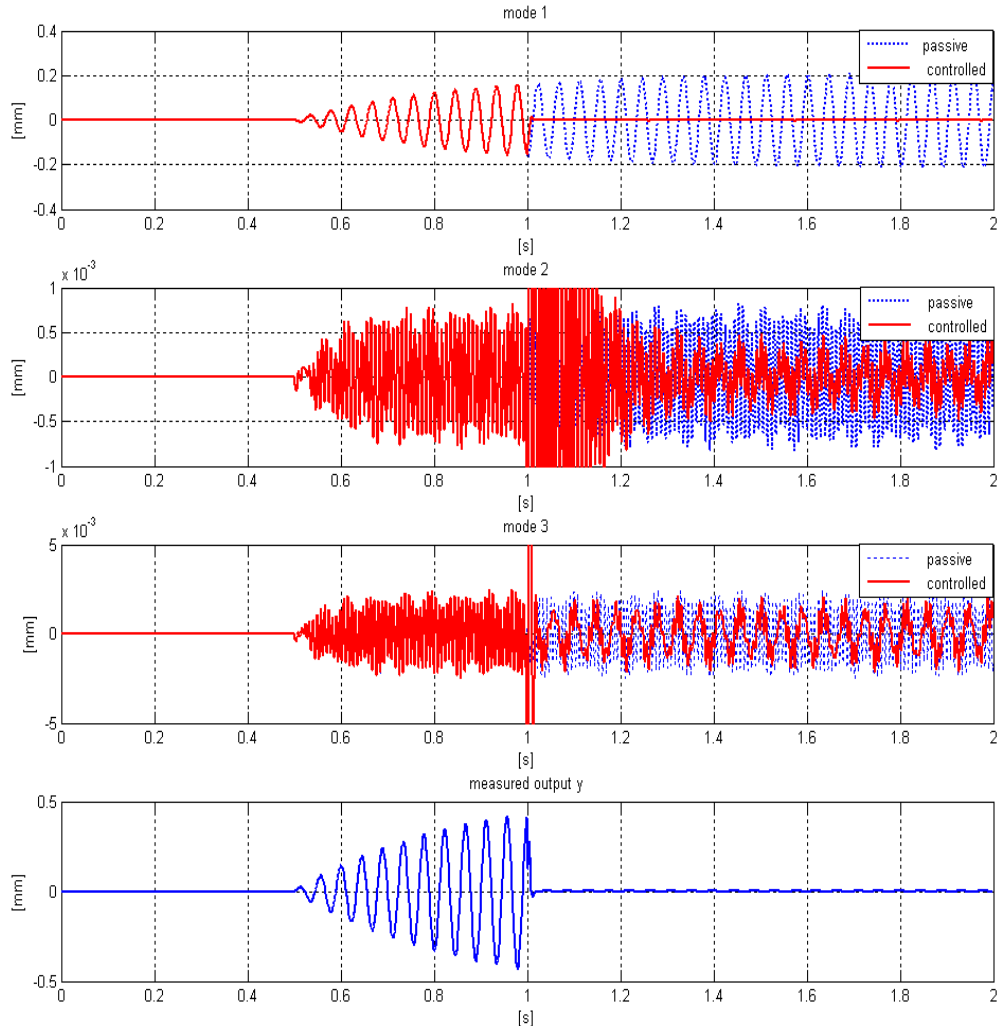


Fig. 3. LQG/LTR with internal model closed loop versus passive time histories

In the next step, the performance of the LQG/LTR with internal model system (25') was tested. The weighting matrices for the controller and filter remained the same as in the relation (27) and we added only one weight for the compensator with the value 10^{11} . For both type of systems we take into account the limitation of the control signal (no higher than ± 500 V). The obtained attenuations for the LQR, respectively LQG/LTR controlled systems were: 42.34, 1.74 and 2.92, respectively 38.31, 6.86 and 3.19 dB (Fig. 3). Once again we can observe that the LQR and LQG/LTR performance are similar. In terms of comparison for the systems with and without internal model, the attenuations are clearly better in the case of using the internal model.

The last set of tests complete the numerical simulations with robustness characteristics testing in the case of the model errors expressed as random uncertainties on modes natural frequencies. The results for both systems, without and with internal model (IM), are presented in the Table 1. As we can see, both systems had similar behavior regarding the robustness property, but the obtained performances are almost twice better for the system with internal model.

Table 1

Results for robustness testing

Nr. crt.	Deviations for mode 1 frequency [%]	Deviations for mode 2 frequency [%]	Deviations for mode 3 frequency [%]	Mode 1 attenuation LTR without IM [dB]	Mode 1 attenuation LTR with IM [dB]	System attenuation LTR without IM [dB]	System attenuation LTR with IM [dB]
1	20	-10	-10	8.33	17.28	8.19	20.49
2	25	-15	-10	6.53	15.46	6.36	18.69
3	25	-10	-15	6.52	15.13	6.32	18.66
4	25	0	-25	6.52	14.37	6.19	18.53
5	25	-25	0	6.54	15.94	6.43	18.40
6	25	25	0	6.53	15.93	6.42	18.70
7	25	25	25	6.54	16.74	6.51	18.67
8	-25	25	25	7.96	17.81	8.10	20.09
9	-25	-25	25	7.96	17.81	8.10	20.09
10	-25	-25	-25	7.91	14.81	8.03	19.90
11	-25	25	-25	7.91	14.8	8.03	19.90
12	-30	-30	30	6.74	16.58	6.9	18.76
13	-40	-40	40	5.01	14.78	5.21	16.80
14	-50	-50	48	3.87	13.48	4.06	15.32
15	-50	-50	50	unstable	unstable	unstable	unstable
16	-50	50	48	3.86	13.44	4.06	15.32
17	50	50	48	1.72	11.14	1.65	12.49
18	50	50	50	1.71	11.17	1.65	12.49
19	50	-50	50	1.72	11.19	1.66	12.49
20	-50	50	50	unstable	unstable	unstable	unstable

All tested systems remained stable with the exception of systems numbered with 15 and 20. In these cases, the condition of decreasing the first frequency coupled with the increasing of the third frequency with 50 percents, seems to induce the worst behavior of systems. Even so, a 50 % deviation from the nominal system can appear only in the cases of health affected systems. Usually, the range of system uncertainties is in practice rounded about $\pm 15\%$. In this range both systems performed, but it can be observed a decreasing attenuation in the case of the system without internal model.

5. Conclusions

The purpose of this study was to develop and evaluate a robust and highly performant integrated LQG/LTR method of control synthesis as applied to a piezo smart composite wing mathematical model in view of vibrations attenuation. Beyond many classical contributions in the field, our approach consists in the proposal of the following two criteria of obtaining the LQG/LTR controller: a) choosing the weight $W(s)$ (18) with a well-defined crossover frequency in correlation with the system dynamics and b) performing a filter gain to satisfy the condition (20).

In fact, the numerical results resumed in the Table 1 can be assumed as a proof of the expected robustness of the LQG/LTR system. Moreover, by introducing an internal model in the controller's design we obtain more robustness properties and remarkable performances.

Thus, the main conclusion of the work concerns the idea of validating the proposed LQG/LTR procedure as an effective methodology of vibrations attenuations for a piezo smart wing.

R E F E R E N C E S

- [1] *I. Ursu and E. Munteanu*, "Piezo smart composite wing with sliding mode control", in Proceedings of CONTROLO 2008 Conference, CD publised ISBN 978-972-669-877-7, pp.166-171, Villa Real, Portugal, 2008.
- [2] *E. Munteanu and I. Ursu*, "Piezo smart composite wing with LQG/LTR control", in Proceedings of IEEE International Symposium on Industrial Electronics, CD publised ISBN 978-1-4244-1666-0, pp.1160-1165, Cambridge, England, 2008.
- [3] *G. Stein and M. Athans*, "The LQG/LTR procedure for multivariable feedback control design", in IEEE Transaction on Automatic Control, vol. **32**, 1987, pp.105–114.
- [4] *A. Isidori, L. Marconi, A. Serrani*, Robust Autonomus Guidance. An Internal Model Approach, in Springer Series, 2003.
- [5] *I. G. Ghionea*, "Optimization approach to conception of a mechanical part using CAD/FEM techniques", in U. P. B. Scientific Bulletin, Series D, Vol. 71, Iss. 4, pp. 43-52, 2009.
- [6] *C. Nguyen and X. Kornmann*, "A comparison of dinamic piezoactuation of fiber-based actuators and conventional PZT paches", in Journal of Intelligent Material Systems and Structures, Vol.**17**, 2006, pp.45-55.

- [7] *N. Mechbal*, “Simulations and experiments on active vibration control of a composite beam with integrated piezoceramics”, in Proceedings of 17th IMACS World Congress, 2005.
- [8] *R. E. Kalman*, “Contributions to the theory of optimal control”, in *Bol. Soc. Mat. Mexicana*, Vol.5, pp.102–109, 1960.
- [9] *I. Postlethwaite, S. Skogestad*, “Robust multivariable control using \mathcal{H}_∞ methods: Analysis, design and industrial applications”, in *Essays on Control – Perspectives in the Theory and its Applications*, Birkhäuser, Boston – Basel – Berlin, 1993.